Memristance controlling approach based on modification of linear M–q curve*

Liu Hai-Jun(刘海军)†, Li Zhi-Wei(李智炜)‡, Yu Hong-Qi(于红旗), Sun Zhao-Lin(孙兆林), and Nie Hong-Shan(聂洪山)

College of Electronic Science and Engineering, National University of Defense Technology, Changsha 410073, *China*

(Received 7 March 2014; revised manuscript received 12 May 2014; published online 24 September 2014)

The memristor has broad application prospects in many fields, while in many cases, those fields require accurate impedance control. The nonlinear model is of great importance for realizing memristance control accurately, but the implementing complexity caused by iteration has limited the actual application of this model. Considering the approximate linear characteristics at the middle region of the memristance-charge (M–q) curve of the nonlinear model, this paper proposes a memristance controlling approach, which is achieved by linearizing the middle region of the M–q curve of the nonlinear memristor, and establishes the linear relationship between memristances M and input excitations so that it can realize impedance control precisely by only adjusting input signals briefly. First, it analyzes the feasibility for linearizing the middle part of the M–q curve of the memristor with a nonlinear model from the qualitative perspective. Then, the linearization equations of the middle region of the M–q curve is constructed by using the shift method, and under a sinusoidal excitation case, the analytical relation between the memristance M and the charge time t is derived through the Taylor series expansions. At last, the performance of the proposed approach is demonstrated, including the linearizing capability for the middle part of the M–q curve of the nonlinear model memristor, the controlling ability for memristance M, and the influence of input excitation on linearization errors.

Keywords: memristor, memristive system, linear model, nonlinear model

PACS: 84.30.Bv, 85.35.–p, 84.32.–y **DOI:** 10.1088/1674-1056/23/11/118402

1. Introduction

At present, the memristor has become a hot issue in physics, materials science, circuits and many other areas.[1–3] In 1971, Chua proved the existence of the memristor from the theoretical viewpoint, and concluded that this device has the memory property of history current.[4] In 2008, the Williams team from HP Laboratories successfully realized nanoscale titanium oxide memristors.[5] Since then, the memristor has attracted widespread attention from researchers.

Owing to the special charge memory characteristics, the memristor has wide potential applications in ultra-high density memory devices,[6,7] chaotic circuits,[8–10] neural networks,[11,12] programmable circuits,[13,14] signal processing,[15,16] and so on. However, memristor modeling is very important for the applications above, and many researchers have done a lot of good work. Strukov *et al.* presented a useful physical model, which is generally called the linear drift model (or linear model), to analyze the characteristics of the actual memristor devices,[5] and then gave a thermophoresis mechanism for explaining unipolar resistive switching in metal–oxide–metal memristors.[17] Yang *et al.* studied the conducting filaments model, and discussed the nature of the filaments and their growth dynamics.[18] Due to the effective solution to the boundary problem and capability for truly simulating the characteristics of real devices, the non-linear model has also attracted widespread attention. Tian *et al.* proposed a compatible circuit model, and discussed the coexistence of the dopant drift and tunnel barrier-based mechanisms[19]. Joglekar and Wolf proposed a nonlinear model with an interesting window function, which could ensure zero drift at the boundaries.[20] Themistoklis *et al.* presented a useful nonlinear dopant drift model that resolved the boundary issues existing in other reported models.[21] However, there exists the problem of implementing complexity caused by iteration when using the nonlinear model, which has limited the actual application of this model. Studies have shown that linear characteristics in the middle region of the memristance-charge (M–q) curve of the nonlinear model memristor would be very useful in practical applications,[11] so it is of great importance for discussing a memristance controlling approach based on the linearization of the middle part of the M–q curve of the nonlinear memristor.

The purpose of this paper is to provide a simple feasible idea for controlling the actual memristor impedances (especially multi-impedances). In discussing impedance control of the nonlinear memristor, the existing literatures usually make use of the window functions based on memristance M and state variable x, considering that the relationships between state variable x and input stimulus are nonlinear iterative, so

*Project supported by the National Natural Science Foundation of China (Grant No. 61171017).

†Corresponding author. E-mail: liuhaijun@nudt.edu.cn

‡Corresponding author. E-mail: lzw89523@gmail.com

© 2014 Chinese Physical Society and IOP Publishing Ltd

it can conclude that the relationship between memristance M and input stimulus are also nonlinear iterative, and we cannot precisely control the memristance M easily by adjusting the input signals. Indeed, the dynamic variation of the inner state in the memristor naturally exhibits nonlinearity. So from the modeling prospect, the nonlinear model has many advantages. However, it is the nonlinearity which makes the impedances of memristors hard to control. Thus, a more easily impedance controlled way is required, and the linearization method could be a good answer. This paper studies the impedance control issue based on memristance M and charge q, by linearizing the middle region of the M–q curve of nonlinear model memristors, and establishes the linear relationship between memristance M and input excitations. The proposed method can achieve multiple impedances control of the intermediate region of the nonlinear memristor, by replacing the iteration operations in hitherto proposed methods. The terminals of the M–q curve are considered as two different resistance states, namely low resistance and high resistance states. With such an idea, we can finally construct an impedance controlled approach with an interesting form of "a straight line and two resistance states".

Considering the approximate linear characteristics at the middle part of the M–q curve of the nonlinear model memristor, this paper proposes a novelty memristance controlling approach. This method, which constructs the linear equations of the middle region of the M–q curve and derives the analytical relation between the memristance M and the charge time t under the sinusoidal excitation case, can provide an alternative solution for the memristor impedance control and other relevant applications.

This paper is organized as follows. Section 2 firstly analyzes the linearization feasibility of the M–q curve of a memristor based on a nonlinear model from the qualitative perspective, then constructs the linear equations of the middle region of the M–q curve by using the shift method, and takes advantage of the Taylor series expansions to derive the analytical relation between the memristance M and the charge time t under the sinusoidal excitation case. In Section 3, some simulations are performed to demonstrate the method's linearizing capability for the M–q curve of a memristor based on a nonlinear model, controlling the ability for memristance M, and the influence of input excitation on linearization errors. Finally, conclusions are given in Section 4.

2. Linearization method for the middle region of the M–q curve of memristor

2.1. Analysis of linear and nonlinear models

This section is used to analyze the linearization feasibility of the M–q curve of the nonlinear model memristor. The symbol of the memristor is shown in Fig. 1(a), and the general definition of polarity is given as: the terminal with a thick black line denotes the negative terminal, and the other side is the positive terminal. When current flows from the positive terminal to the negative terminal, the memristor goes into the state of low resistance $R_{\rm ON}$, and when current flows from the negative terminal to the positive terminal, the memristor goes into the state of high resistance $R_{\rm OFF}$. Figure 1(b) shows the linear model of the TiO_2 memristor.[5] TiO_{2-x} denotes the doped layer while TiO_2 represents the undoped layer, and these two layers are sandwiched between two metal contacts Pt. Let the thickness of the TiO_{2-x} region be $w(t)$, which is generally called the state variable. Let the thickness of the sandwiched area be D.

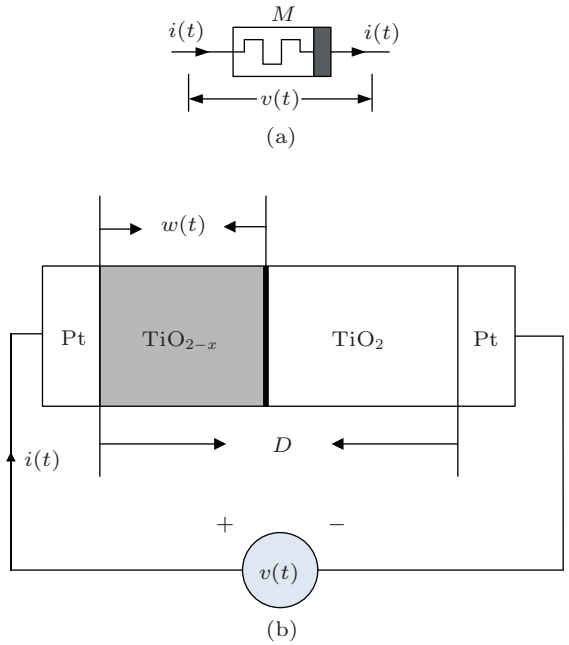


Fig. 1. (color online) The sketch map of the memristor. (a) Symbol of memristor; (b) linear model of the TiO_2 memristor.

The relation between the voltage and the current is computed as[5]

$$v(t) = \left(R_{\rm ON}\frac{w(t)}{D} + R_{\rm OFF}\left(1 - \frac{w(t)}{D}\right)\right) i(t). \tag{1}$$

The memristance $M(t)$ is calculated

$$M(t) = R_{\rm OFF} + \frac{(R_{\rm ON} - R_{\rm OFF})}{D} w(t). \tag{2}$$

From the circuit theory, we can obtain the relation between the charge $q(t)$ and the current $i(t)$ as follows:

$$q(t) = \int_0^t i(\tau)\,{\rm d}\tau. \tag{3}$$

In the condition of linear model,[5] the state variable $w(t)$ can be obtained by

$$\frac{{\rm d}w(t)}{{\rm d}t} = \mu_{\rm V}\frac{R_{\rm ON}}{D} i(t), \tag{4}$$

where μ_V denotes the average dopant mobility. The integral of Eq. (4) is shown

$$w(t) = \mu_V \frac{R_{ON}}{D} q(t) + w_0, \tag{5}$$

where w_0 is the initial thickness of the doped layer. Substituting Eq. (5) into Eq. (2), we can get the expression of the memristance $M_L(t)$ as Eq. (6), where the subscript L represents the linear model of memristors

$$M_L(t) = R_{OFF} + \frac{\mu_V R_{ON}(R_{ON} - R_{OFF})}{D^2} q(t) + \frac{(R_{ON} - R_{OFF}) w_0}{D}. \tag{6}$$

The nonlinear model can be constructed based on the linear model,[5] and the main difference of these two models is reflected in the expression of the state variable. The state variable $w(t)$ of the nonlinear model can be computed by multiplying the right side of Eq. (4) with a window function $F_p(w)$,[20]

$$\frac{dw(t)}{dt} = \mu_V \frac{R_{ON}}{D} i(t) F_p(w). \tag{7}$$

It is noticed that there are many kinds of window functions for memristors based on the nonlinear model; in this paper, we use the following window function proposed by Joglekar and Wolf:[20]

$$F_p(w) = 1 - \left(2\frac{w(t)}{D} - 1\right)^{2p}, \tag{8}$$

where p is the nonlinearity parameter. Combining Eq. (8) with Eq. (7), we cannot achieve the analytical solution of Eq. (7), so $w(t)$ can only be calculated by using iterative methodology[11,20]

$$w(t + \Delta T) \approx \mu_V \frac{R_{ON}}{D} \left(1 - \left(2\frac{w(t)}{D} - 1\right)^{2p}\right) \Delta q + w(t), \tag{9}$$

$$\Delta q = \int i(t) dt = I \Delta T, \tag{10}$$

where Δq represents the charge increment field to the memristor during the time interval ΔT. It is noted that when computing the Δq using Eq. (10), the input current $i(t)$ during a small time interval ΔT can be seen as a constant value I.

Substituting Eqs. (9) and (10) into Eq. (2), we can obtain the relation between the memristance $M_{NL}(t)$ and the charge $q(t)$, where the subscript NL denotes the nonlinear model of memristors

$$M_{NL}(t + \Delta T) \approx R_{OFF} + \frac{\mu_V R_{ON}(R_{ON} - R_{OFF}) \Delta q}{D^2} \left(1 - \left(2\frac{w(t)}{D} - 1\right)^{2p}\right) + \frac{(R_{ON} - R_{OFF}) w(t)}{D}. \tag{11}$$

Figure 2 demonstrates the M–q curves for the linear and nonlinear models of memristors. It is noticed that the M–q curve for the linear model is expressed by using Eq. (6), while that for the nonlinear model is represented by Eq. (11) with three different nonlinear parameters $p = 1, 2, 3$. The parameters of the memristor itself and the external excitation are the same as those in Section 3.1. From Fig. 2, it can be seen that the M–q relation for the linear model is linear, while in the condition of the nonlinear model, the M–q curve is curvilinear. With the increase of the nonlinearity parameter p, the linear trends of the nonlinear curves become obvious, and the middle part of the nonlinear curves can be approximated as a straight line. Similar conclusions can be seen in Ref. [11]. Hence, we can try to use the linear equations for describing the middle region of the M–q curve of memristors based on the nonlinear model, while for the other regions of this curve, we can consider them as two different resistance states, namely the state of low resistance and high resistance, unlike the states of the middle part. By using this idea, we can construct an approach for impedance controlling with an interesting form of "a straight line and two resistance states". It is noticed that when controlling impedances with the method above, we should firstly determine two impedance thresholds M^H (the high resistance state) and M^L (low resistance state) at terminals, according to the given impedance controlled error ε_M. When the actual controlled memristance M_r is less than M^L, the memristor is considered to be in a low-impedance state. On the contrary, when the actual controlled memristance M_r is higher than M^H, the memristor is considered to be in a high-impedance state. As a result, a border control problem arises, that is, when the actual impedance M_r is within the low border and high border, how to make the memristance precisely return to an expected impedance state M_e (between M^L and M^H). A feasible way is to apply inverted current firstly to the memristor with continuously reading the memristance values until its resistor arrives at one value between M^L and M^H, then we can get the relationship between actual controlled impedance M_r and charge

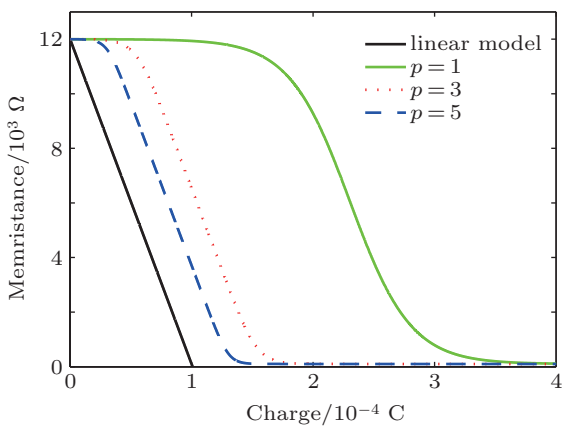


Fig. 2. (color online) The M–q curves for the linear and nonlinear models of memristors.

q and use this proposed linearization method to achieve precise control from M_r to the expected impedance M_e. It is noted that the proposed method in this paper is very simple and effective for multiple impedances control of actual memristors.

2.2. Linearization method for the middle region of the *M–q* curve of the memristor

Considering the approximate linearity characteristics of the middle region of the M–q curve for the nonlinear model, this section constructs the linear equations of the middle part of the M–q curve by using the shift method, and takes advantage of the Taylor series expansions to derive the analytical relation between the memristance M and the charge time t under a sinusoidal excitation case.

Supposing that the memristance values of the low and high resistance states are R_{ON} and R_{OFF} respectively, and the applied excitation is $i(t) = I_{max}\sin(\omega t)$, where I_{max} is the amplitude of the input current and ω denotes the frequency of the current. The implementation of the linearization method for the middle region of the M–q curve is described in detail as follows.

Step 1 Apply the input excitation $i(t) = I_{max}\sin(\omega t)$ to the memristor. When $M'_{NL} = R_{OFF}/2$, record the excitation time τ and use Eq. (3) to calculate the charge q'_{NL}

$$q'_{NL} = \frac{I_{max}\left(1-\cos(\omega\tau)\right)}{\omega}. \tag{12}$$

Step 2 Substitute Eq. (12) into Eq. (6), and calculate the memristance M'_L under the circumstance of a linear model.

Step 3 Compute the memristance difference of two different models $\Delta M = M'_{NL} - M'_L$, and modify Eq. (6) to obtain the linear equation of the middle part of the M–q curve for a nonlinear model as follows:

$$\begin{aligned} M(t) &= R_{OFF} + \frac{\mu_V R_{ON}\left(R_{ON}-R_{OFF}\right)}{D^2}q(t) \\ &\quad + \frac{\left(R_{ON}-R_{OFF}\right)w_0}{D} + \Delta M. \end{aligned} \tag{13}$$

It is obvious to see that the relation between $M(t)$ and $q(t)$ is linear. Because equation (13) is the linear simplification of the middle region of the M–q curve for the nonlinear model memristor, there must exist linearization errors. For the given memristance error ε_M, by substituting Eqs. (11) and (13) into

$$|M(t) - M_{NL}(t)| \le \varepsilon_M, \tag{14}$$

we can compute the lower bound q^L and upper bound q^U of the charge $q(t)$ satisfying the error condition ε_M.

Under the case of given input excitation, it is an important way to control the excitation time t for realizing accurate memristance states. In order to achieve the memristance value easily and accurately, we also derive the analytical relation between the memristance M and the charge time t under a sinusoidal excitation case. The specific realization is described as follows.

Supposing that the impedance value of the memristor at time t is M. Combining Eq. (12) with Eq. (13), we can obtain

$$\begin{aligned} M &= R_{OFF} + \frac{I_{max}\mu_V R_{ON}\left(R_{ON}-R_{OFF}\right)}{D^2\omega}\left(1-\cos(\omega t)\right) \\ &\quad + \frac{\left(R_{ON}-R_{OFF}\right)w_0}{D} + \Delta M. \end{aligned} \tag{15}$$

Let

$$a = R_{OFF} + \frac{\left(R_{ON}-R_{OFF}\right)w_0}{D} + \Delta M, \tag{16}$$

$$b = \frac{I_{max}\mu_V R_{ON}\left(R_{ON}-R_{OFF}\right)}{D^2\omega}, \tag{17}$$

$$x = \omega t. \tag{18}$$

From the known conditions, we can see that a and b are constants, and equation (15) can be simplified as

$$M = a + b\left(1-\cos(x)\right). \tag{19}$$

The Taylor series expansions of $\cos(x)$ is given as

$$\cos(x) = 1 - \frac{x^2}{2!} + \frac{x^4}{4!} - \cdots = 1 - \frac{x^2}{2!} + \frac{x^4}{4!} + O(x^4), \tag{20}$$

where $O(x^4)$ represents the Peano remainder. It is noticed that equation (20) is established in the condition that x is small enough and $\cos(x)$ is continuous with the differentiability at $x = 0$.

Considering the computational simplicity and accuracy, by substituting the first three items of Eq. (20) into Eq. (19), we can obtain

$$(x^2-6)^2 = \frac{24(a-M)+36b}{b}. \tag{21}$$

Taking into account the boundary conditions of the nonlinear model and the non negative characteristic of time parameter t, we can solve Eq. (21) as follows:

$$x = 6 - \sqrt{\frac{24(a-M)+36b}{b}}. \tag{22}$$

Combining Eq. (22) with Eq. (18), we can further obtain the excitation time t corresponding to the memristance M. Substituting Eqs. (15)–(22) into Eq. (14), we can easily calculate the lower bound t^L and upper bound t^U of the excitation time t satisfying the error condition ε_M.

3. Simulations

Three experiments are given to verify the effectiveness of the proposed linearization method. The first one is used to validate the linearization capability of the proposed method; the second one is utilized to examine whether the linearization method can control the memristance exactly; and the last one is performed to analyze the impact of input excitations on linearization ability. Assume that the nonlinear model memristor, whose parameters are set to be $R_{ON} = 100\ \Omega$, $R_{OFF} = 12\ \text{k}\Omega$,

$D = 10$ nm, $\mu_V = 10^{-14}$ m^2/V·s and $w_0 = 10^{-3}$ nm, can be excited by a source of harmonic current $i(t) = I_{max}\sin(\omega t)$. The nonlinear model makes use of the form as Eq. (8) with the nonlinearity parameter $p = 5$, namely $F_{p=5}(w)$. It is noticed that, in order to describe the change process of the memristance of the nonlinear memristor more clearly, w_0 is set to be a small value. Nevertheless, its value does not affect the performance of the proposed linearization method.

3.1. Linearization capability for the middle region of the *M–q* curve

The input excitation is set to be $i(t) = I_{max}\sin(\omega t)$ with $I_{max} = 1$ mA and $\omega = 1$ rad/s. By using the linearization method proposed in Section 2.2, we can compute $\Delta M = 3.611$ kΩ, and then obtain for the M–q curve of the nonlinear model memristor with $F_{p=5}(w)$

$$M(t) = 1.561 \times 10^4 - 1.19 \times 10^8 \times q(t). \tag{23}$$

Figure 3 shows the linearization capability for the M–q curve of the nonlinear model memristor. It is noticed that in Fig. 3(a), the dash dot line represents the M–q curve of the linear model, the solid line denotes the M–q curve of the nonlinear model with $F_{p=5}(w)$, and the dotted line is the linearized M–q curve of the nonlinear model. From Fig. 3(a), it can be seen that the linearized M–q curve is in agreement with the middle region of the M–q curve of the nonlinear model. The solid line in Fig. 3(b) demonstrates the linearization errors of the nonlinear model with $F_{p=5}(w)$. From this figure, it can be seen that the middle part of the error curve is approximately linear and located close to zero, so we can deduce that the linear equation (23) can well describe the intermediate portion of the nonlinear model with $F_{p=5}(w)$. It can also be seen that for the other part of the nonlinear model, the linearization errors are large, that is because the nonlinear phenomena of the two M–q curve terminals of the nonlinear model are very obvious (as shown in Fig. 3(a)). It is noticed that in practical applications, we can consider the terminal regions, which are different from the middle regions of the M–q curve, as two different resistance states, namely the state of low resistance and high resistance. The dotted line in Fig. 3(b) shows the linearization errors of the nonlinear model with $F_{p=5}(w)$ under the condition of $\varepsilon_M = 50$ Ω. Using Eq. (14), we can compute the lower bound $q^L = 3.983 \times 10^{-5}$ C and upper bound $q^U = 1.208 \times 10^{-4}$ C of the charge $q(t)$ satisfying the error condition ε_M. Substituting Eqs. (15)–(22) into Eq. (14), we can also calculate the lower bound $t^L = 0.2832$ s and upper bound $t^U = 0.4967$ s of the excitation time t corresponding to the charge $q(t)$ above. It is noticed that the real charge time corresponding to the lower bound q^L and upper bound q^U of the charge $q(t)$ are also exactly 0.2832 s and 0.4967 s separately. So this experiment, to a certain degree, verifies that the linearization method can realize accurate control of the memristance values, by using the analytical relationship between the memristance M and excitation time t.

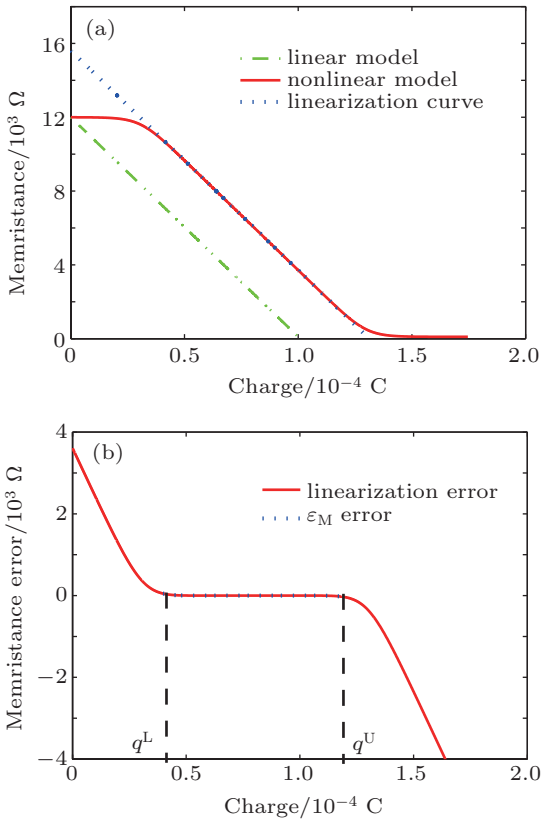


Fig. 3. (color online) The linearization capability for the M–q curve of the nonlinear model memristor. (a) Linearization for the M–q curve; (b) linearization errors.

3.2. Control capability of the memristance

This section is used to validate the memristance control capability of the proposed method. The parameters of the input excitation are the same as those in Section 3.1. By using Eq. (23), this experiment tries to realize nine different memristances, namely 10 kΩ, 9 kΩ, 8 kΩ, 7 kΩ, 6 kΩ, 5 kΩ, 4 kΩ, 3 kΩ, and 2 kΩ. Through Eqs. (15)–(22), we compute the corresponding excitation time as 0.3080 s, 0.3348 s, 0.3595 s, 0.3827 s, 0.4046 s, 0.4254 s, 0.4454 s, 0.4645 s, and 0.4829 s, respectively. Figure 4 shows the linearization errors of the nine different required memristances.

From Fig. 4, it can be seen that the memristance errors, which are corresponding to the seven different memristances (9 kΩ, 8 kΩ, 7 kΩ, 6 kΩ, 5 kΩ, 4 kΩ, and 3 kΩ), are less than 0.25 Ω, namely 0.002% of the maximum memristance of the memristor. Among these seven memristances, the memristance error corresponding to 6 kΩ is minimum and is approximately equal to zero. That is because 6 kΩ is just the mean value of the maximum memristance and the proposed linearization method takes the mean point as the transformation reference point. From Fig. 4, it can also be seen that the

memristance errors corresponding to 10 kΩ and 2 kΩ, which are approximately equal to 5.6 Ω and 7.2 Ω respectively, are larger than those of the other seven memristances. That is because the nonlinear phenomena of the two M–q curve terminals of the nonlinear model is obvious, and the proposed linearization method focuses on controlling the memristances of the middle part of the M–q curve. However, the linearization errors corresponding to 10 kΩ and 2 kΩ are still less than 0.06% of the maximum memristance of the nonlinear memristor. Therefore, it can be concluded that the linearization method proposed in this paper has a better control capability of the memristances in the middle region, while for the other regions (for example, the required memristances are larger than 10 kΩ or less than 2 kΩ), the memristances can be classified into two different resistance states, namely the state of low resistance and high resistance.

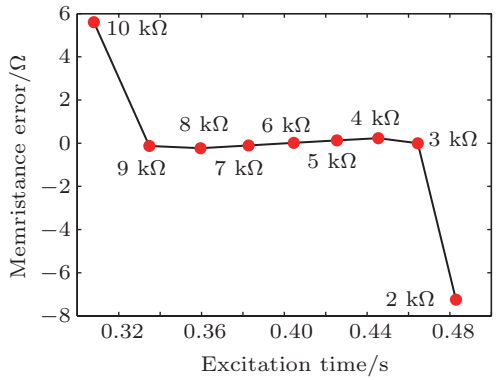


Fig. 4. (color online) The memristance control capability of the linearization method.

3.3. Influence of the input excitation on linearization ability

Considering that the input excitation is set to be a source of harmonic current $i(t) = I_{\max}\sin(\omega t)$, this section is performed to analyze the impact of the input excitation on the linearization errors and the excitation time, in the condition of the input current with different amplitude $I_{\max}$ and frequency ω. There exist two experiments. The first one simulates the impact of the input excitation current, which is with a constant amplitude $I_{\max}$(1 mA) and five different frequencies ω (0.5 rad/s, 1 rad/s, 2 rad/s, 4 rad/s, and 8 rad/s), on the linearization ability. The influence of the input excitation with different frequencies on linearization ability can be seen in Fig. 5.

Figure 5(a) demonstrates the linearization errors in the condition of $\varepsilon_{\mathrm{M}} = 50\ \Omega$. It can be seen that the linearization error curves of different frequencies are almost the same, namely, the effects on linearization errors caused by frequency changes can be almost ignored. Figure 5(b) shows the distribution of the excitation time corresponding to different frequencies in the condition of $\varepsilon_{\mathrm{M}} = 50\ \Omega$, and the figures in different rectangles (dashed line) denote the corresponding lengths of the excitation time intervals satisfying the error condition $\varepsilon_{\mathrm{M}} = 50\ \Omega$. It can be seen that with the increase of the frequency ω, the lower bound, upper bound and interval length of the corresponding excitation time decrease gradually. So it can get the conclusion that the frequency changes can affect the charging time of the nonlinear memristor. As shown in Section 2.2 above, equation (20) is established under the condition that x is small enough and $\cos(x)$ is continuous with the differentiability at $x = 0$. We can also deduce from Eq. (18) that the variable x is proportional to the frequency ω. In such a situation, a feasible way for precise memristance control requires the control accuracy of the excitation time t to be small enough to ensure that the variable x can be maintained at a lower value.

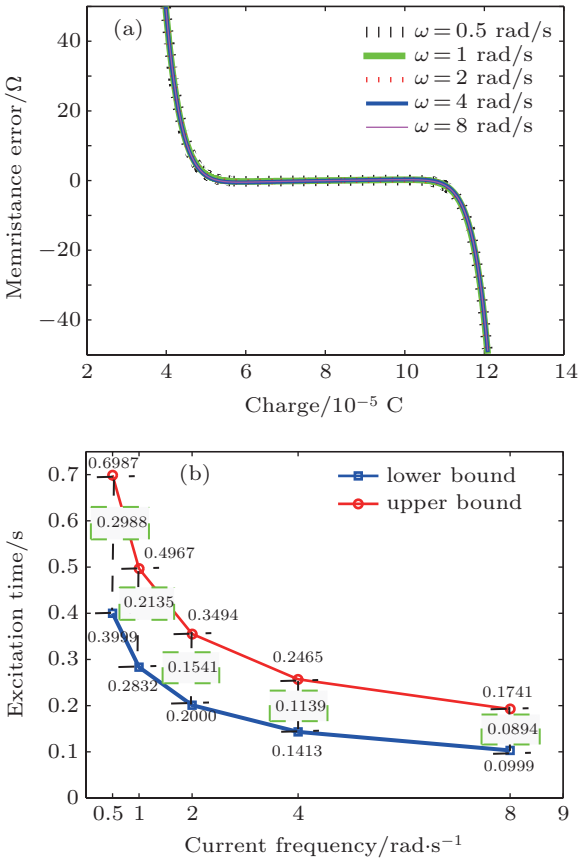


Fig. 5. (color online) Influence of the input excitation with different frequencies on linearization ability. (a) Linearization errors in the condition of $\varepsilon_{\mathrm{M}} = 50\ \Omega$; (b) the distribution of excitation time in the condition of $\varepsilon_{\mathrm{M}} = 50\ \Omega$.

The second experiment analyzes the influence of the input excitation with five different amplitudes on the linearization ability. The input current is set to be with four different amplitudes $I_{\max}$(1 mA, 2 mA, 4 mA, and 8 mA) and a constant frequency ω (1 rad/s). The influence of the input excitation with different amplitudes on linearization ability can be seen in Fig. 6.

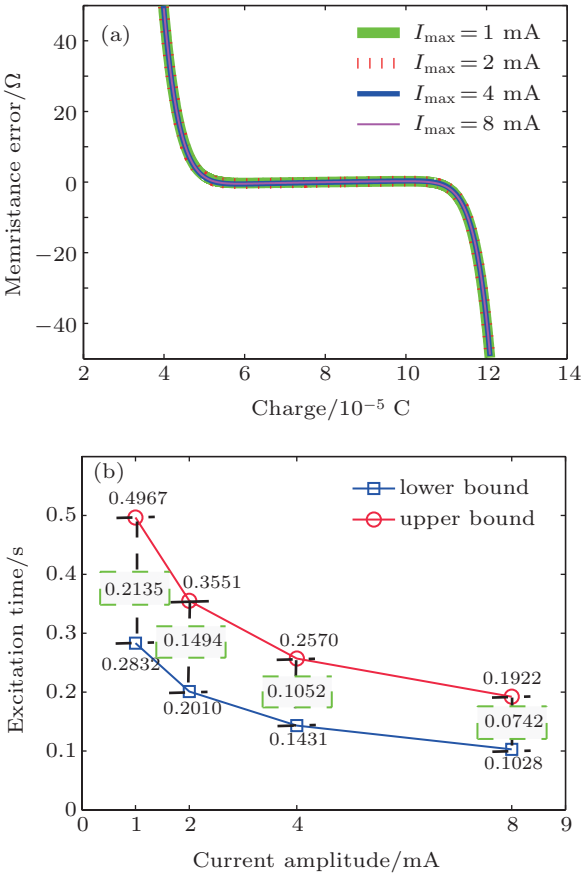


Fig. 6. (color online) Influence of the input excitation with different amplitudes on linearization ability. (a) Linearization errors in the condition of $\varepsilon_M = 50\ \Omega$; (b) the distribution of excitation time in the condition of $\varepsilon_M = 50\ \Omega$.

Figure 6(a) demonstrates the linearization errors in the condition of $\varepsilon_M = 50\ \Omega$. It can be seen that the linearization error curves of different amplitudes are almost the same, namely, the effects on linearization errors caused by amplitude changes can be almost ignored. Figure 6(b) shows the distribution of the excitation time corresponding to different amplitudes in the condition of $\varepsilon_M = 50\ \Omega$, and the figures in different dashed line rectangles denote the corresponding lengths of the excitation time intervals satisfying the error condition $\varepsilon_M = 50\ \Omega$. It can be seen that with the increase of the amplitude I_{max}, the lower bound, upper bound and interval length of the corresponding excitation time also decrease gradually. So it can conclude that the changes of the input excitation current can also influence the charging time of the nonlinear memristor.

From the two experiments above, we can see that the effects on linearization errors, caused by the changes of frequencies and amplitudes of the input excitation current, can be almost ignored. But the changes of these two factors can influence the charging time of the nonlinear memristor obviously.

4. Conclusions

This paper proposes a memristance controlling approach, by linearizing the middle region of the M–q curve of the nonlinear model memristor. For the terminal regions of the mentioned curve, we can consider the corresponding memristances as two different resistance states, namely the state of low resistance and high resistance. Simulation results show that the proposed method has a good linearizing capability for the middle part of the M–q curve and accurate controlling ability for memristances. Although the effects on linearization errors caused by the changes of frequencies and amplitudes of the input excitation current can be ignored, the influence caused by the changes of two such factors on the charging time of the nonlinear memristor is obvious. This study could offer an alternative solution for controlling memristor impedances and other relevant applications.

References

[1] Slipko V A, Pershin Y V and Di Ventra M 2013 *Phys. Rev. E* **87** 042103
[2] Liu H J, Li Z W, Bu K, Sun Z L and Nie H S 2014 *Chin. Phys. B* **23** 048401
[3] Li Z W, Liu H J and Xu X 2013 *Acta Phys. Sin.* **62** 96401 (in Chinese)
[4] Chua L O 1971 *IEEE Trans. Circ. Theory* **18** 507
[5] Strukov D B, Snider G S, Stewart D R and Williams R S 2008 *Nature* **453** 80
[6] Jung C, Choi J and Min K 2012 *IEEE Trans. Nanotechnol.* **11** 611
[7] Eshraghian K, Kyoung-Rok C, Kavehei O, Soon-Ku K, Abbott D and Sung-Mo S K 2011 *IEEE Transactions on Very Large Scale Integration Systems* **19** 1407
[8] Iu H H C, Yu D S, Fitch A L, Sreeram V and Chen H 2011 *IEEE Trans. Circ. Sys.* **58** 1337
[9] Bao B C, Hu W, Xu J P, Liu Z and Zou L 2011 *Acta Phys. Sin.* **60** 120502 (in Chinese)
[10] Sun J, Shen Y, Zhang G, Wang Y and Cui G 2013 *Chin. Phys. B* **22** 040508
[11] Kim H, Sah M, Yang C, Roska T and Chua L O 2012 *IEEE Trans. Circ. Sys.* **59** 148
[12] Howard G, Gale E, Bull L, de Lacy Costello B and Adamatzky A 2012 *IEEE Transactions on Evolutionary Computation* **16** 711
[13] Tian X B and Xu H 2013 *Chin. Phys. B* **22** 088501
[14] Pershin Y V and Di Ventra M 2010 *IEEE Trans. Circ. Sys.* **57** 1857
[15] Shin S, Kim K and Kang S M 2012 *Electron. Lett.* **48** 78
[16] Merrikh-Bayat F, Shouraki S B and Rohani A 2011 *IEEE Transactions on Fuzzy Systems* **19** 1083
[17] Strukov D B, Alibart F and Williams R S 2012 *Appl. Phys. A* **107** 509
[18] Yang Y, Gao P, Gaba S, Chang T, Pan X and Lu W 2012 *Nat. Commun.* **3** 732
[19] Tian X B, Xu H and Li Q J 2013 *Chin. Phys. B* **22** 088502
[20] Joglekar Y N and Wolf S J 2009 *Eur. J. Phys.* **30** 661
[21] Prodromakis T, Boon P P, Papavassiliou C and Toumazou C 2011 *IEEE Transactions on Electron Devices* **58** 3099